SHAPE EFFECT ON SEISMIC ENERGY ABSORPTION CAPACITY OF HYSTERETIC DAMPER FOR K-BRACED FRAME

Hiroyuki TAMAI[1], Kazuo KONDOH[2], Yoshikazu KITAGAWA[3] And Masami HANAI[4]

SUMMARY

In this paper, a new type of the K-braced frame with shear resistance member is shown as a hysteretic damper. The required shape and stiffenings of the panel in the shear resistance member are investigate through material-geometrical nonlinear analyses of the panel under repeated in-plane shear loading, so as to prevent a rapid deterioration of its hysteresis loops due to shear buckling in the panel. On the basis of the analytical results, loading tests on the shear resistance members, which have a low yield point steel panel and an ordinary steel panel with cut tee stiffeners, are carried out. From the experimental results, it is clarified that the adequate stiffenings of the panel lead to obtain its excellent characteristics in plastic deformation and energy absorption capacity as a hysteretic damper.

INTRODUCTION

Present authors have developed a new braced frame with shear resistance member made of a panel and four surrounding flange plates [1-3]. The shear resistance member prevents the brace buckling and absorbs the seismic energy into the plastic shear deformation of the panel in the member, so that improves the seismic resistance characteristics of the braced frame structure. Since the panel in the hysteretic damper is strained large, repeated shear deformation under severe earthquake, it might cause plastic shear buckling in the panel, which leads to the deterioration of its hysteresis loop, when the width-to-thickness ratio of the panel is set up relatively large. In order to function effectively as a damper, the shape and the stiffenings of the panel must be selected stiff enough that there is no deterioration of hysteresis loop of the panel.

In this paper, from these viewpoints, material-geometrical nonlinear analyses of relatively thick panel subjected to large, repeated in-plane shear force are performed to investigate the shape of the panel, which prevents the rapid deterioration of its hysteresis loops due to shear buckling. Also, on the basis of the analytical results, the shear resistance members, which have a low yield point steel panel and an ordinary steel panel with cut tee stiffeners, are prepared as a good candidate for a hysteretic damper. The loading tests on the shear resistance members are carried out to verify the improvement in plastic deformation and energy absorption capacity by use of the simple stiffenings in the panel.

BRACED FRAME WITH HYSTERETIC DAMPER

Braced frame with damper

The proposed K-braced frame with the damper is shown in Fig. 1.
The K-brace with the damper consists of a K shaped uneccentric brace with a shear resistance member and two link plates between the upper beam and the joint beam. The shear resistance member (S.R.M.) is made of a panel and four surrounding steel flanges. The proposed braced frame has a function of truss having high horizontal

[1] *Dept of Structural Engineering, Hiroshima Univ., Japan Email:tamrix@ipc.hiroshima-u.ac.jp*
[2] *Dept of Structural Engineering, Hiroshima Univ., Japan Email:tamrix@ipc.hiroshima-u.ac.jp*
[3] *Dept of Structural Engineering, Hiroshima Univ., Japan Email:tamrix@ipc.hiroshima-u.ac.jp*
[4] *Department of Architecture, Kinki University, Higashi-Hiroshima City, Japan E-mail: j-hana@arch.hiro-kindai.ac.jp*

stiffness for loads such as a strong wind and moderate earthquake and also has a function of hysteretic damping device absorbing seismic energy effectively by means of shear yielding of the panel in the S.R.M. for load such as a severe earthquake. It is possible to reduce the responses of the building frame so as to give no serious damage to the frame under a severe earthquake, and easily repair the braced frame only by renewing the shear resistance member after the earthquake.

Shear resistance member

The two types of shear resistance members (S.R.M.), installed in the present K-braced frame, are shown in Fig. 2. The one of S.R.M. is made of a low yield point steel panel and surrounding four ordinary steel flanges attached by welding. The other is made of an ordinary steel panel with cut tee stiffeners and the same surrounding four flanges. The panel is touched with flanges of cut tee.
Because low yield point steel, used in the member, has very low yield stress (about 80-98(MPa)), it is possible to design the S.R.M. so that the width-to-thickness ratio of the panel is less than about 30, without excess of the required strength and the shear deformation angle of the member. On the other hand, the cut tee stiffenings restrain the panel from out-of-plane deflection satisfactorily. Because the cut tees are only touched with the panel, which is subjected to large plastic deformation, there is no excessive concentration of plastic strain in the panel as compared with the ordinary stiffeners that attached with the panel by welding. Both types of S.R.M. are possible to set the panel stiff enough to prevent shear buckling of the panel under alternately repeated large shear loading.
Under a severe earthquake, before the brace buckling, the panel yields without plastic shear buckling for the repeated shear deformation. Therefore, the shear resistance member will possess excellent deformation and energy absorption characteristics.

POST BUCKLING BEHAVIOR OF STEEL PANEL UNDER IN-PLANE SHEAR LOADING

A rapid deterioration of hysteresis loop of the shear resistance member is caused by shear buckling in the panel.
In order to investigate the shape of the panel, which prevents a rapid deterioration of its hysteresis loop due to shear buckling, geometrical nonlinear analyses of elasto-plastic rectangular plate subjected to in-plane shear force are performed on the cases under monotonic and cyclic reversed loading.

Analysis procedures and analyzed

The analyzed model and finite element model are shown in Fig.3 and Fig.4, respectively.
A target of analysis is relatively thick steel panel, which plastic shear buckling occurs under alternately repeated in-plane shear loading. Panel thickness of S.R.M. is relatively so thick that we must take account of out-of-plane shear ingredient.
The features of the numerical procedures, employed in this study, to trace the elasto-plastic and geometrical nonlinear behaviors of thick panel, are summarized as follows.

i) Eight/nine nodes element [4,5], based on Mindlin plate theory, which has 3 displacement parameters (u, v, w) and 2 rotation parameters (θ x, θ y) a node, is used.
ii) Selective reduced integration [6] is used in evaluation of out-of-plane shear strain energy, to avoid the shear locking, occurred in case of thin plate.
iii) Layered approach is used when we evaluate the stiffness distribution in direction of thickness. Stresses and strains, including out-of-plane shear ingredient, are evaluated at layered subdomains, and total stiffness of the section is calculated as the sum of subdomain's stiffness.
iv) Yield condition and hardening rule are adopted von Mises criterion and Ziegler's kinematic hardening rule [7], respectively.
v) Incremental and iterative method of Newton-Raphson type is used as numerical technique for solving nonlinear equations.
vi) Arc length method of Ramm type with radial return constraint [8] is used to determine the load and displacement increment. It is possible to stabilize the solution after shear buckling with partially unloading.
vii) Explicit integration method with radial correction is used to get stress distribution at subdomains. It is possible to keep the stress point on the yield locus under yielding.

In this study, the panel is assumed to be clamped on each side (See Fig.3(c)). Also, external load is given by the prescribed displacement on the top side of the panel. Imperfection of the panel is introduced as initial deflection: w_o by Eq.(1).

$$w_0 = w_a \cdot \cos(\frac{\pi \cdot x}{a}) \cdot \cos(\frac{\pi \cdot y}{b}) \quad (1)$$

where, w_a : amplitude of initial deflection, a, b : side long of the panel
In order to evaluate the concentration of plastic strain under combined stresses, an equivalent plastic strain: $\varepsilon^{(p)}_{eq}$ is calculated by Eq.(2).

$$\varepsilon^{(p)}_{eq} = \int d\varepsilon^{(p)}_{eq} \quad (2.a)$$

where,

$$d\varepsilon^{(p)}_{eq} = \frac{2}{\sqrt{3}} \cdot (d\varepsilon^{(p)2}_{x} + d\varepsilon^{(p)}_{x} \cdot d\varepsilon^{(p)}_{y} + d\varepsilon^{(p)2}_{y} + \frac{1}{4} \cdot d\gamma^{(p)2}_{xy} + \frac{1}{4} \cdot d\gamma^{(p)2}_{yz} + \frac{1}{4} \cdot d\gamma^{(p)2}_{zx})^{\frac{1}{2}} \quad (2.b)$$

and $d\varepsilon^{(p)}_{x}, d\varepsilon^{(p)}_{y}, d\gamma^{(p)}_{xy}, d\gamma^{(p)}_{yz}, d\gamma^{(p)}_{zx}$ are components of plastic strain increments.

Loading programs are two types as follows; (1) The monotonic loading, in which (δ/b) is increased to 0.05 (rad) monotonically. (2) Cyclic reversed loading, in which the amplitude (δ/b) is constant to 0.05 (rad) and the loading is repeated 4 cycles. In case of monotonic loading, influence of the imperfection, the in-plane shear strength, the shape of the panel on elasto-plastic behavior are studied. Series of analyses are the cases, which amplitude of initial deflection: w_a , yield stress: σ_y and width-to-thickness ratio:(a/t) of the panel are changed (t/5, t/10, t/100, t/1000), (98, 147, 196, 245, 294, 343 (MPa)) and (20, 30, 40, 50, 60, 80, 100), and the cases, which aspect ratio :(a/b) of the panel is changed (1.0,1.2,1.5,2.0,3.0) in a/t=50,100 , respectively.
On the other hand, in case of cyclic loading, influence of the shape of the panel on development of shear buckling is studied. A series of analysis is the cases, which (a/t) is changed (30, 40, 50).
Unless we mentioned the specific condition, following conditions would be adopted as standard ones.

$$w_a = t/100, \quad a/b = 1.0, \quad a/t = 100, \quad a = 25(cm)$$
$$E_t / E = 1/100, \quad E = 20.57(GPa), \quad \nu = 0.28, \quad \sigma_y = 98(MPa) \quad (3.a\text{-}h)$$

Analyses results and discussion

The results show in Figs.5-12.
Figs.5, 6, 8, 10, 11 show the relation between the shear force: Q normalized by its yield load: Q_y $(=a \cdot t \cdot \sigma_y / \sqrt{3})$ and the shear displacement: d normalized by the panel length: b in solid line, and the relation between (Q/Q_y) and the lateral deflection at the center of the panel: $w^{(c)}$ normalized by its thickness: t in break line.
Figs.7, 9, 12 show the relation between (Q/Q_y) and maximum equivalent plastic strain overall the panel: $\varepsilon^{(p)}_{eqmax.}$
From these results, it is clarified that;

(1) Imperfection of the panel is affected sensitively on the load carrying capacity.
(2) The lower yield stress panel is used, the smaller maximum equivalent plastic strain is observed. As a result, the better energy absorption capacity is obtained.
(3) The yield stress: σ_y and width-to-thickness ratio: (a/t) are set to 98 (MPa) and 50, respectively, there is no shear buckling and no degradation of its strength under monotonic loading.
(4) In accordance with increasing aspect ratio: (a/b), the central deflection $w^{(c)}$ tends to decrease in any (a/t). Once the strength of the panel degrades when $(w^{(c)}/t)$ reaches about 0.5, and then its strength increases after the deflection is large enough to develop the tension field.
(5) In case of cyclic loading, if (a/t) and σ_y is less than 40 and 98 (MPa) and the number of cycle is below 4.0, the deflection: $w^{(c)}$ does not increase and the perfect spindle-shaped hysteresis loop is observed. On the contrary, if (a/t) is more than 50, $w^{(c)}$ is accumulated after first cycle, the deterioration of its hysteresis loop is observed in accordance with increasing the number of cycle.

IMPROVEMENT IN ENERGY ABSORPTION CAPACITY DUE TO SHAPE EFFECT

On the basis of analytical results, full-scale shear resistance members, which have simple panel stiffenings, are prepared. In order to verify the improvement of the seismic performance, the monotonic and cyclic reversed loading tests are performed.

Outline of loading tests

The test specimens and the test setup are shown in Figs.2, 13.

The shear resistance member (S.R.M.) is jointed L-shaped beams by friction bolts. L-shaped beams are pin-connected with the lever and the buttress. During the tests, compressive and tensile forces act on the S.R.M. through L-shaped beam, and the S.R.M. is kept in shear strained, which is the same loading condition as the one installed in the present K-braced frame. The loading capacity of the present test system is enhanced three times as much as the one of actuators by use of a lever action.

The test specimens are prepared three types as follows; (a) a low yield point steel panel (LYP100, a/t=19.8) jointed with flanges (SS400, t=12(mm), 19(mm))(LN specimen) and (b) an ordinary steel panel (SS400, a/t=39.7) with cut tee panel stiffeners jointed with the same flanges (SS specimen) (c) an ordinary steel panel (SS400, a/t=39.7) without panel stiffener jointed with the same flanges (SN specimen).

All specimens are annealed under 780^{o}C ,2hrs to improve the brittleness on heat affected zone by welding.

The results of material tests using the same material, thickness and heat treatment as the S.R.M. are shown in Table 1. Loading measurement is the shear force acting on S.R.M.: Q_s, which is derived from the load cells installed on the head of digital actuators. Displacement measurements are the shear displacement of the S.R.M.: δ, which is obtained as the averaged value from the front and rear instruments, and the lateral deflection of the panel (at 3/8 of its height from the bottom of panel on center line): $w^{(d)}$ (See Fig.14).

The loading programs are two types as follows; (1) the monotonic loading, which increase shear displacement: δ monotonically up to 3.0 (cm), (2) the cyclic reversed loading, in which the amplitude of shear displacement: δ is constant to 1.5(cm).

In this study, the critical use limit of the damper is defined at the point where the strength of S.R.M. decreases to 0.9 to its maximum strength. The total absorbing energy: W_p, number of half cycle: N_f , when strength of S.R.M. reaches 0.9 of its maximum strength, are calculated as an index of energy absorption capacity.

Test results and discussion

Test results show in Figs.15-18 and Table 2.

Fig.15 shows the relation between the shear force of S.R.M.: Q_s and the shear displacement: δ normalized by the panel length: b, and the relation between Q_s and the lateral deflection of the panel: $w^{(d)}$ normalized by the panel thickness under monotonic loading. Fig.16 shows the relation between Q_s and (δ /b) under cyclic reversed loading. Fig.17 shows the relation between amplitude of shear load of S.R.M.: Q_{sa} and number of half cycle under cyclic reversed loading. Fig.18 shows the crack patterns after the cyclic reversed loading test. Table 2 shows total absorbed energy: W_p, fatigue life: N_f and maximum strength: Q_{samax} of S.R.M. under cyclic reversed loading.

From these results, it is clarified that;

(1) Each specimen has small elastic limit shear displacement and excellent plastic deformation capacity. Strength of SN specimen degrades after δ=2.4(cm) because of shear buckling in the panel under monotonic loading.
(2) The strength of SN specimen rapidly degrades in accordance with increasing number of loading cycle. On the contrary, LN, SS specimens hold high strength for cyclic reversed loading, number of half cycle until failure of LN, SS specimens are three and a half times as long as the one of SN specimen.
(3) In LN, SS specimen, there is no shear buckling. After the end of vertical flanges being cracked, the crack developed in toe of the panel welding, and then these strengths degrade. On the contrary, in SN specimen, remarkable shear buckling is observed in first cycle, and then its strength degrades. The crack developed in the center of the panel in diagonal directions.

CONCLUSIONS AND REMARKS

The material-geometrical nonlinear F.E.M. analyses and loading tests are performed on the shear resistance member (hysteretic damper). The obtained results in the present study are summarized as follows;

i) Imperfection of the panel is affected sensitively on its load carrying capacity, when the shear buckling occurs in the panel.
ii) The lower yield stress panel is used, the more concentration of plastic strain due to shear buckling is relaxed. Consequently, the better energy absorption capacity is obtained.
iii) If the width-to-thickness ratio and the yield stress of the panel are set less than 40 and 98 (MPa), respectively, it is possible to prevent the plastic shear buckling and the rapid deterioration of its hysteresis loop under cyclic shearing.
iv) The adequate stiffenings in the panel such as the cut tee panel stiffener or the low yield point thick panel leads to obtain its excellent characteristics in plastic deformation and energy absorption capacity as a hysteretic damper.

REFERENCES

[1] Tamai, H., Takenaka,H., Nakano, T., Kojima,O. ,Kondoh,K. ,Hanai, M. (1991):"On hysteretic damper using low yield stress steel plate installed in K-braced frame (Part I) Outline of the device and its mechanism", Summaries of technical papers of annual meeting AIJ, Series C, pp.1447-1448.
[2] Tamai, H., Takenaka, H., Kondoh, K., Nakamura,Y., Hanai, M.(1994):"Application of low yield stress steel to K-braced frame with hysteretic damper", Steel construction engineering, JSSC, Vol.1, No.2, pp.41-52.
[3] Tamai,H., Kondoh,K., Hanai,M. ,Iwaoka,S., Ryujin,H., Fujinami,T.(1998):"Panel stiffening effect on energy absorbing capacity of the hysteretic damper made of SS400 steel", Journal of structural enginnering , Vol.44B, pp.493-502.
[4] Tamai,H., Kondoh,K. ,Hanai,M.(1998):"A h-adaptive mindlin plate element and its application to thick panel subjected to repeated in-plane shear force", Proc. of Int. Conference on Comp. Eng. Sci., Modelling and simulation based engineering, Atlanta, USA, Vol.1, pp.790-795.
[5] Hughes, T.J.R., Liu, W.K.(1981): "Nonlinear finite element analysis of shells ", Comp. Meth. Appl. Mech. Eng. , Vol.26, pp.331-362.
[6] Hughes, T.J.R. , Taylor, R.L. , Kanoknukulchai, W. (1977) : "A simple and efficient finite element for plate bending", Int. J. Num. Mech. Eng., Vol.11, pp.1529-1543.
[7] Ziegler, H. (1959) : "A modification of Prager's hardening rule", Q.Appl.Mech.", Vol.17, No.1, pp.55-65.
[8] Noguchi,H., Hisada,T.(1992): "Development of sensitivity analysis method in post buckling problems", J. of J.S.M.E., Series A, Vol.58, No.556, pp.2415-2422.

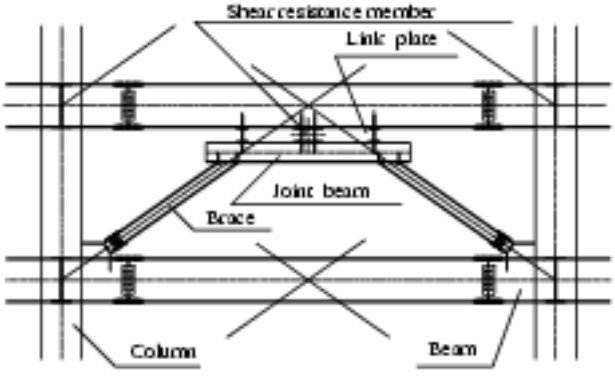

Fig.1 Present hysteretic damper in K-braced frame

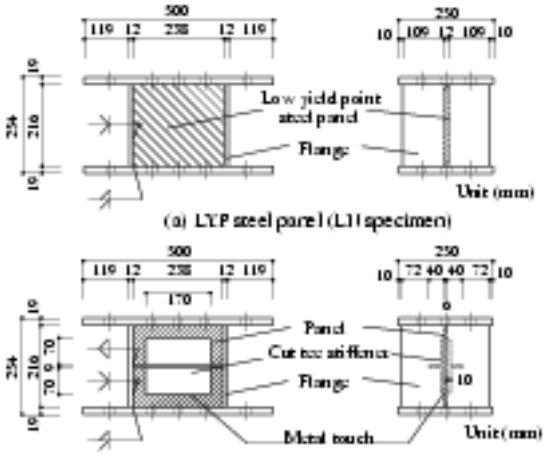

Fig.2 Detail of two types of hysteretic dampers (shear resistance member)

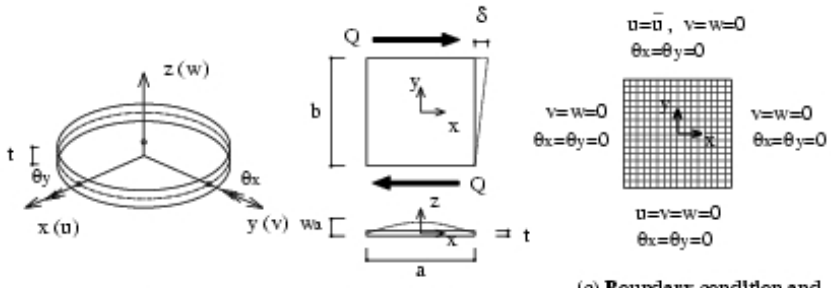

(a) Co-ordinate system (b) Analyzed model (c) Boundary condition and mesh division

Fig.3 Analyzed panel subjected to in-plane shear loading

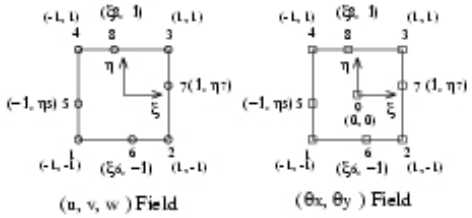

(u, v, w) Field (θx, θy) Field

Fig.4 Mindlin shell element [4] adopted in present study

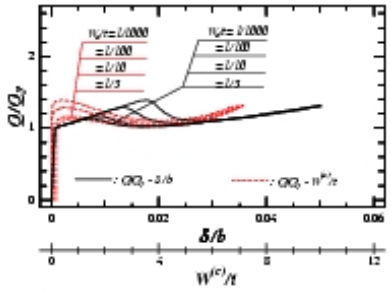

Fig.5 Influence of imperfection on (load - shear disp.), (load - lateral deflection) relations

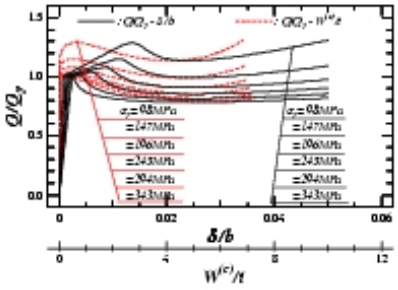

Fig.6 Comparison of (load - shear disp.), (load - lateral deflection) relations with yield stress

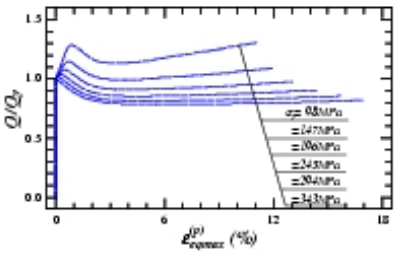

Fig.7 Comparison of (load - maximum equivalent plastic strain) relations with yield stress

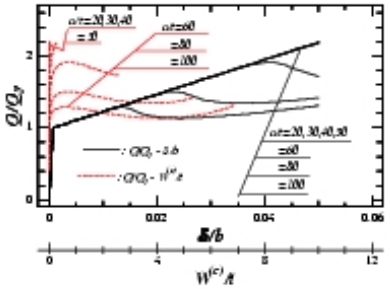

Fig.8 Comparison of (load - shear disp.), (load - lateral deflection) relations with width-to-thickness ratio

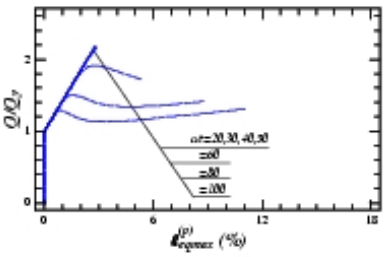

Fig.9 Comparison of (load - maximum equivalent plastic strain) relations with width-to-thickness ratio

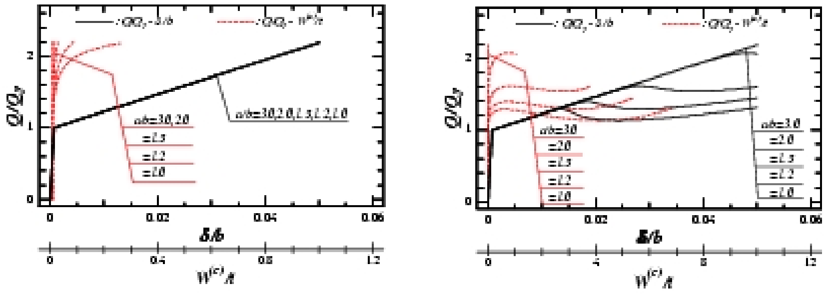

(a) a/t = 50 (b) a/t=100

Fig.10 Comparison of (load - shear disp.), (load - lateral deflection) relations with aspect ratio

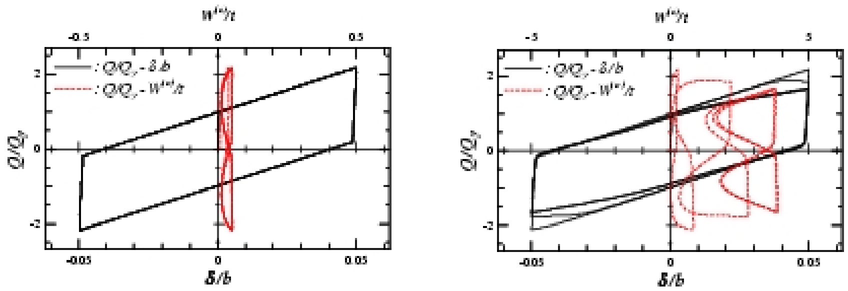

(a) a/t = 40 (b) a/t=50

Fig.11 (Load - shear disp.), (load - lateral deflection) relations under cyclic reversed loading

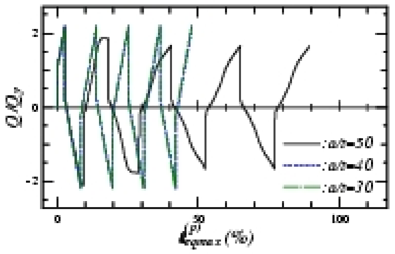

Fig.12 (Load - maximum equivalent plastic strain) relations under cyclic reversed loading

Table 1 Mechanical properties of materials used in test specimen

Type	t	E	σ_y	σ_u	ε_u	H_R	Usage
	mm	GPa	MPa	MPa	%	HR	
SS400	6.0	202.7	193	287	55.1	40.7*	Panel SS,SN
	12.0	202.7	303	474	46.5	72.6*	Flange SN,LN,SS
LYP100	12.0	199.5	83	249	70.7	65.9**	Panel LN

t : Thickness, E : Young's modulus, σ_y : Nominal yield stress

σ_u : Nominal ultimate strength, ε_u : Elongation

H_R : Rockwell hardness(*:Scale-B for SS400, **:Scale-F for LYP100)

All material were annealed under 780°C, 2hrs.

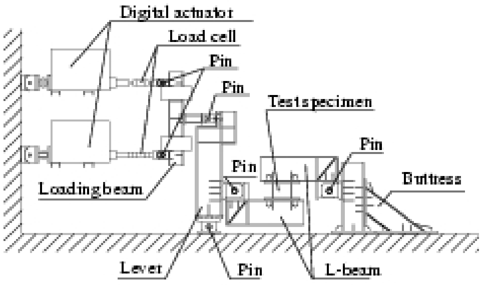

Fig.13 Loading test apparatus

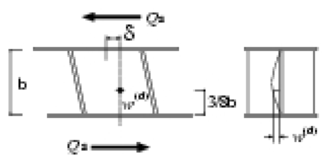

Fig.14 Schematic illustrations of measured values

7

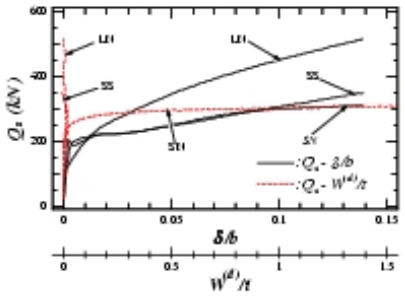

Fig.15 (Load - shear disp.) and (Lateral deflection - shear disp.) relations under monotonic loading

Table 2 Absorbed energy, fatigue life and maximum strength of shear resistance member under cyclic reversed loading

Specimen	W_p	N_f	Q_{zumax}
	kJ	*H.C.*	*kN*
SN	157.0	19.5	355.7
LN	1101.7	69.5	643.9
SS	694.9	59.5	433.2

Wp : Absorbed Energy, *Nf*: Fatigue life, *Qsumax*: Maximum strength
H.C. : Half cycle

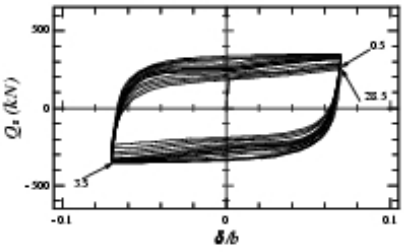

Fig.16(a) (Load - shear disp.) relation under cyclic reversed loading (SN specimen)

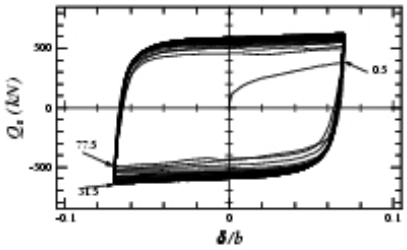

Fig.16(b) (Load - shear disp.) relation under cyclic reversed loading (LN specimen)

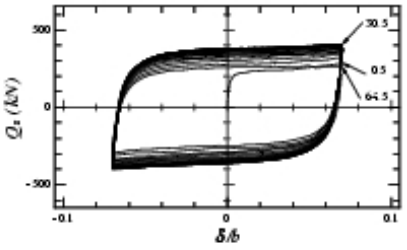

Fig.16(c) (Load - shear disp.) relation under cyclic reversed loading (SS specimen)

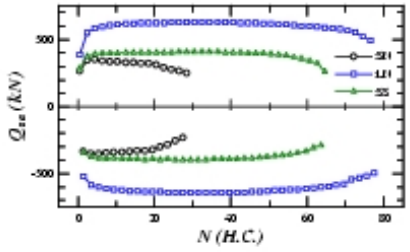

Fig.17 Amplitude of load - number of half cycle relation under cyclic reversed loading

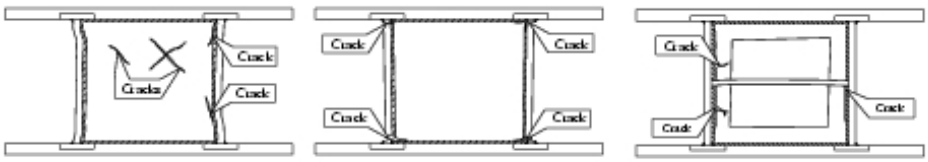

(a) SN specimen (b) LN specimen (c) SS specimen

Fig.18 Crack patterns after cyclic reversed loading test